Zika and chikungunya viruses decrease salivation in *Aedes aegypti* mosquitoes

Lucie SOURIAC[1], Mateus BERNI[1], Benjamin VOISIN[2], Thiago H.J.F. LEITE[1,3], Eric MAROIS[1], Fabien AUBRY[4] and João T. MARQUES[1]

Affiliations

[1] Inserm U1257, CNRS UPR9022, University of Strasbourg, Strasbourg, France

[2] CNRS UPR3572, University of Strasbourg, Strasbourg, France

[3] Department of Biochemistry and Immunology, Instituto de Ciências Biológicas, Universidade Federal de Minas Gerais, Belo Horizonte/MG, Brazil

[4] CNRS UPR9022, University of Strasbourg, Strasbourg, France

Abstract

Aedes mosquitoes transmit viruses of global health concern through blood feeding. While biting, mosquitoes inject viruses but also saliva factors that modulate feeding and potentially viral transmission. However, studying this interplay is limited by our ability to quantify saliva release. Here, we developed a transgenic *Aedes aegypti* line that secretes fluorescent markers in saliva, enabling visualization of probing sites on human skin explants and quantification of salivation. Saliva secretion remained robust under diverse physiological conditions but was significantly reduced upon Zika or chikungunya virus infection. Nevertheless, virus release did not correlate with levels of saliva factors, suggesting decreased salivation does not lower chances of viral transmission. Our results bring perspective to the previously described increase in probing behavior in infected mosquitoes, indicating it may be caused by lower release of saliva factors. Thus, the negative impact of infection on salivation may have been selected to facilitate virus transmission.

Main text

Introduction

Every year worldwide, mosquitoes are the deadliest animal for humans due to the pathogens they vector. Arboviruses such as yellow fever (YFV), dengue (DENV), Zika (ZIKV) or chikungunya (CHIKV) are transmitted by *Aedes* mosquitoes. Current global warming and urbanization dynamics facilitate the spread of mosquitoes in temperate regions, increasing the risk of arboviruses circulation in these areas[1,2]. If no efficient measures are taken, 60% of the world population is expected to become at risk to contract DENV by the year 2080[2]. In this study, we focus on the principal vector of arboviruses, *Ae. aegypti*, which is well adapted to urban landscapes and feeds preferentially on humans[3,4]. It is established in tropical and subtropical regions of the world, allowing the endemic spread of mosquito-borne viruses in these regions[5–8]. To prevent future outbreaks, one level of action is to improve our understanding of the biology of the mosquito vector allowing the development of novel strategies to decrease virus transmission.

Mosquitoes get infected when they take a blood meal on an infected vertebrate host. Virus acquired in the blood infects enterocytes in the midgut before crossing the gut epithelial barrier and disseminating to the hemocoel of the mosquito[9]. Once in the circulation of the mosquito, the virus will infect and replicate in the salivary glands[10] allowing it to be released when the mosquito is probing on its next host to blood feed. Notably, in the infected salivary gland, the virus segregates in specific vesicles at the apical cavity of secretory acinar cells prior to secretion, seemingly distinct from secretory vesicles[11]. Since the virus is released from the salivary glands during probing, it is however assumed that transmission is intimately associated with the release of saliva factors by the mosquito[12]. Indeed, these factors have an important role when mosquitoes probe and blood feed on a vertebrate host, being involved in the inhibition of host responses as well as feedback loops that fine-tune mosquito behavior, for example modifying proboscis morphology and proprioception signaling to promote feeding on a vertebrate host[12,13]. Moreover, venom allergen-1 and sialokinin present in the saliva indirectly increase the pathogenicity of ZIKV by activating autophagy or vascular leakage at the biting site, respectively[14,15]. The D7 saliva protein interacts directly with DENV particles, inhibiting infection[16], while aegyptin activates immune responses in mice, decreasing DENV infection[17].

Natural biting of a mosquito vector affects the pathogenesis of arboviruses compared to injection of the virus artificially, alone or coupled with salivary gland extracts (SGE) to mimic the presence of saliva components[18,19]. These results reinforce a role of mosquito saliva in modulating arbovirus infection in the mammalian host. However, past studies have mostly taken advantage of artificial models, co-injecting saliva factors or salivary gland extracts together with the virus[20,21]. Indeed, tracking the release of saliva factors and virus by an infected mosquito remains a challenge. Numerous studies have analyzed salivation measurements in viral transmission assays using forced salivation, where mosquitoes are immobilized and allowed to salivate in drops of oil[22,23] or tips filled with physiological

buffers[24]. These have mostly relied on indirect estimations of the release of saliva factors analyzing the volume of saliva released or engorgement of the mosquito. These technical limitations prevent us from understanding the connection between salivation and virus transmission. These may also help explain why these strategies underestimate the amount of transmitted virus compared to natural feeding on mice[25,26].

Here, we developed a transgenic *Ae. aegypti* reporter line expressing epitope-tagged fluorescent proteins in the distal-lateral lobes of the salivary glands that are also secreted in the saliva. This line allowed us to quantify the release of saliva factors at the resolution of individual mosquitoes and to characterize basic aspects of the physiology of salivation. Finally, this line allowed us to study the correlation between salivation and transmission of two relevant arboviruses, ZIKV and CHIKV.

Results

Generating a transgenic mosquito line to track salivation

To generate a mosquito line that expresses a reporter for salivation, we first searched for genes encoding proteins secreted within the saliva. The 30Ka (AAEL010228 encoding SAAG-4) and 30Kb (AAEL010235 encoding aegyptin) genes are controlled by a bidirectional promoter that drives their expression in the distal-lateral lobes of *Ae. aegypti* salivary glands[27,28]. The 30Kb gene is also expressed in the proximal-lateral lobes to a lesser extent[27]. Using the recent Mosquito Cell Atlas[29], we confirmed that 30Ka and 30Kb are specifically expressed in the distal-lateral lobes of the salivary gland of *Ae. aegypti* mosquitoes and the proximal lobes in the case of 30Kb (**Figure 1a,b**). They were among the top 35 expressed genes in the distal-lateral lobes of the salivary glands (**Supplementary table 1**). Significant expression of 30Ka and 30Kb was not detected in other mosquito tissues (**Supplementary figure 1a**). The SAAG-4 and aegyptin proteins, encoded by 30Ka and 30Kb genes, respectively, are among the top 20 most abundant secreted in the saliva[30,31]. Mass spectrometry analyses show that SAAG-4 and aegyptin are also in the top 10 proteins found in salivary gland extracts[16]. Of note, the 30K promoter has been used to successfully drive specific transgene expression in the salivary gland of mosquitoes[32,33], but not to track salivation. Here we built a construct with the 30K promoter maintaining the signal peptides encoded by 30Ka and 30Kb genes in fusion with the fluorescent markers mTurquoise (mTurq) and Yellow Fluorescent Protein (YFP), respectively (**Figure 1c**). V5 and HA epitope tags were also inserted to facilitate detection of mTurq and YFP, respectively (**Figure 1c**). dsRED was used as a marker for transgenesis driven by a ubiquitous promoter (AAEL003888, poly-Ubiquitin, pUb) on the same piggyBac construct (**Figure 1c**), which was randomly inserted into the genome. A mosquito line with a single insertion that was mapped to a non-coding locus on the 3rd chromosome was selected (**Figure 1c** and **Supplementary figure 1b,c**; see methods for details). This line, named Fudgel, was further characterized.

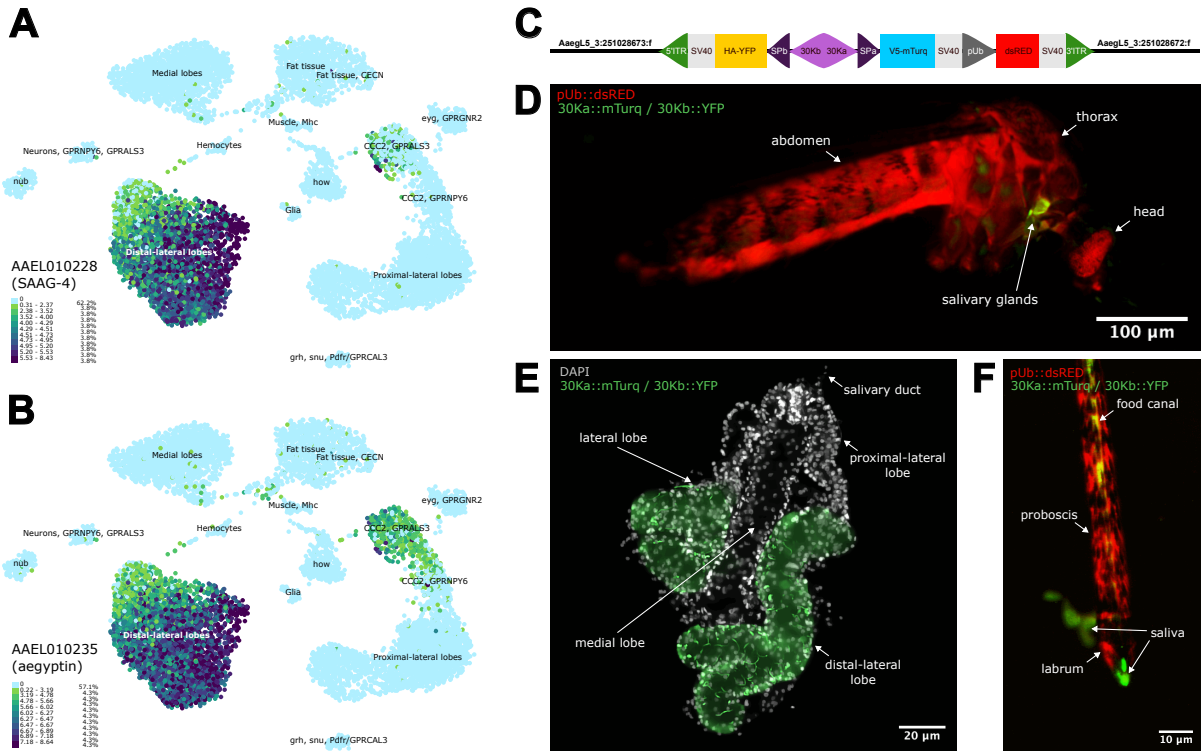

Figure 1- Establishment and phenotypic characterization of the Fudgel transgenic line

A-B) UMAP representation of 30Ka (AAEL010228/SAAG-4) (**A**) and 30Kb (AAEL010235/aegyptin) (**B**) expression patterns in *Ae. aegypti* snRNAseq data from salivary glands generated with the UCSC Cell Browser (Goldman et al. 2025). **C**) Fudgel transgene genetic construct and insertion locus in the Ae. aegypti Bangkok genome. The construct is composed of the bidirectional 30K promoter (30Ka and 30Kb) and their associated endogenous signal peptides (purple and dark purple). 30Ka drives the expression of the mTurq gene tagged in 5' with a V5 tag and followed by a SV40 transcription terminator (blue and grey). 30Kb drives the expression of the YFP gene tagged in 5' with a HA tag and followed by SV40 (yellow and grey). dsRED is used as a transgenesis reporter and expressed ubiquitously with a pUb (AAEL003888/poly-Ubiquitin) promoter, and is followed by SV40 (dark grey, red and grey). The construct is flanked by Inverted Terminal Regions (ITRs) derived from piggyBac transposons and used for transgenesis (Olmo et al. 2018). The insertion locus of the transgene was identified by Inverse PCR. **D-F**) Expression patterns of the mTurq/YFP (green) and dsRED (red) fluorescent markers in whole body (**D**), salivary gland (**E**) and proboscis (**F**) of Fudgel mosquitoes. Nuclei stained with DAPI are shown in **E**.

Characterizing mosquito salivation using the Fudgel reporter line

The analysis of mosquitoes from the Fudgel line on a fluorescent microscope with a green filter - which does not differentiate YFP and mTurq - revealed fluorescent labeled tissue in the mosquito thorax, where the salivary glands are expected to be (**Figure 1d**). In contrast, the dsRED fluorescent marker, whose expression is driven by a ubiquitous promoter, labeled the whole mosquitoes (**Figure 1d**). In dissected salivary glands from Fudgel mosquitoes, green labelling was observed in the distal-lateral

129 lobes (**Figure 1e**) as expected using the 30k promoter. By confocal microscopy, YFP and mTurq
130 expression can be seen in the salivary glands with distinct patterns (**Supplementary Figure 1d)**. Of
131 note, YFP had a broader expression pattern confirming previous observations that 30Kb is also
132 expressed in proximal-lateral lobes while 30Ka had a more restricted expression[27]. On a fluorescent
133 microscope, we noted that the mTurq signal was more intense than YFP. For further fluorescent imaging
134 acquisitions, exposure time for YFP was increased by a 10-fold to allow detection similar to mTurq. This
135 may be due to a genomic position effect of the piggyBac insertion, since 30Kb is more expressed than
136 30Ka[29], and aegyptin is more abundant in saliva than SAAG-4[14]. Nevertheless, the expression pattern
137 of the fluorescent proteins in the salivary gland was as expected based on the promoters we used.
138 Since the signal peptides encoded by 30Ka and 30Kb are retained in the construct, we next analyzed
139 the presence of the fluorescent markers in the saliva itself. Fluorescent saliva could be observed in
140 green, blue and yellow channels inside the food canal of the proboscis while the walls of the canal are
141 labelled with dsRED (**Figure 1f** and **Supplementary figure 1d**). A real-time video shows release of the
142 mTurq fluorescent marker during salivation on a Petri dish (**Supplementary video 1**). These results
143 suggest that the mosquito line produces fluorescent markers in the salivary glands and secretes them
144 in the saliva. Although the markers are specifically produced by the distal-lateral lobes, proteins from
145 all lobes are equally represented in the saliva (**Supplementary table 2**)[14,29]. Therefore, the release of
146 the fluorescent markers should allow direct tracking of salivation.
147
148 To quantitatively monitor the release of saliva factors by individual mosquitoes, we measured levels of
149 fluorescent markers by western blot using a forced salivation protocol (**Figure 2a**). V5-mTurq could be
150 readily detected after 30 minutes of forced salivation in about half of the mosquitoes tested (**Figure**
151 **2b,c**; **Supplementary figure 2** and raw data in **Supplementary table 3**). Neither the marker levels nor
152 the proportion of individuals with detectable markers - together referred to as salivation performance -
153 changed significantly at 0.5, 1 and 2 hours of forced salivation (**Figure 2c**). Of note, HA-YFP was not
154 detected by western blot (**Figure 2b**) consistent with the microscopy results that suggested it is not as
155 abundant as V5-mTurq. Since V5-mTurq allows us to quantify saliva factors, we next analyzed the
156 salivation performance of individual mosquitoes at different stages of completion of their gonotrophic
157 cycle. Blood-fed Fudgel mosquitoes were analyzed at different days post-feeding (dpf) (7 dpf, 10 dpf or
158 14 dpf) with or without egg laying compared to sugar-fed individuals (**Figure 2d**). Overall, the
159 physiological state of the mosquito did not affect salivation performance (**Figure 2e**; **Supplementary**
160 **figure 3** and raw data in **Supplementary table 4**). There was a significant decrease in saliva levels at
161 10 dpf in mosquitoes that were allowed to lay eggs and thus completing their gonotrophic cycle (**Figure**
162 **2e**). This tendency at day 10 was observed in three out of four independent replicates indicating a
163 physiological difference rather than experimental variation (**Supplementary figure 4**). This observation
164 is in agreement with previous reported variations in host seeking and blood feeding behavior at different
165 stages of the gonotrophic cycle[34]. We also quantified levels of the fluorescent marker remaining in the
166 salivary glands after salivation (**Figure 2f**). No significant differences in markers levels - mTurq and
167 YFP - were observed in salivary glands, compared to control mosquitoes after blood-feeding on mice
168 or forced salivation (**Figure 2g; Supplementary figure and table 5**). These results suggest that levels

of saliva factors released in both natural and artificial salivation settings are relatively small compared to what remains in the glands.

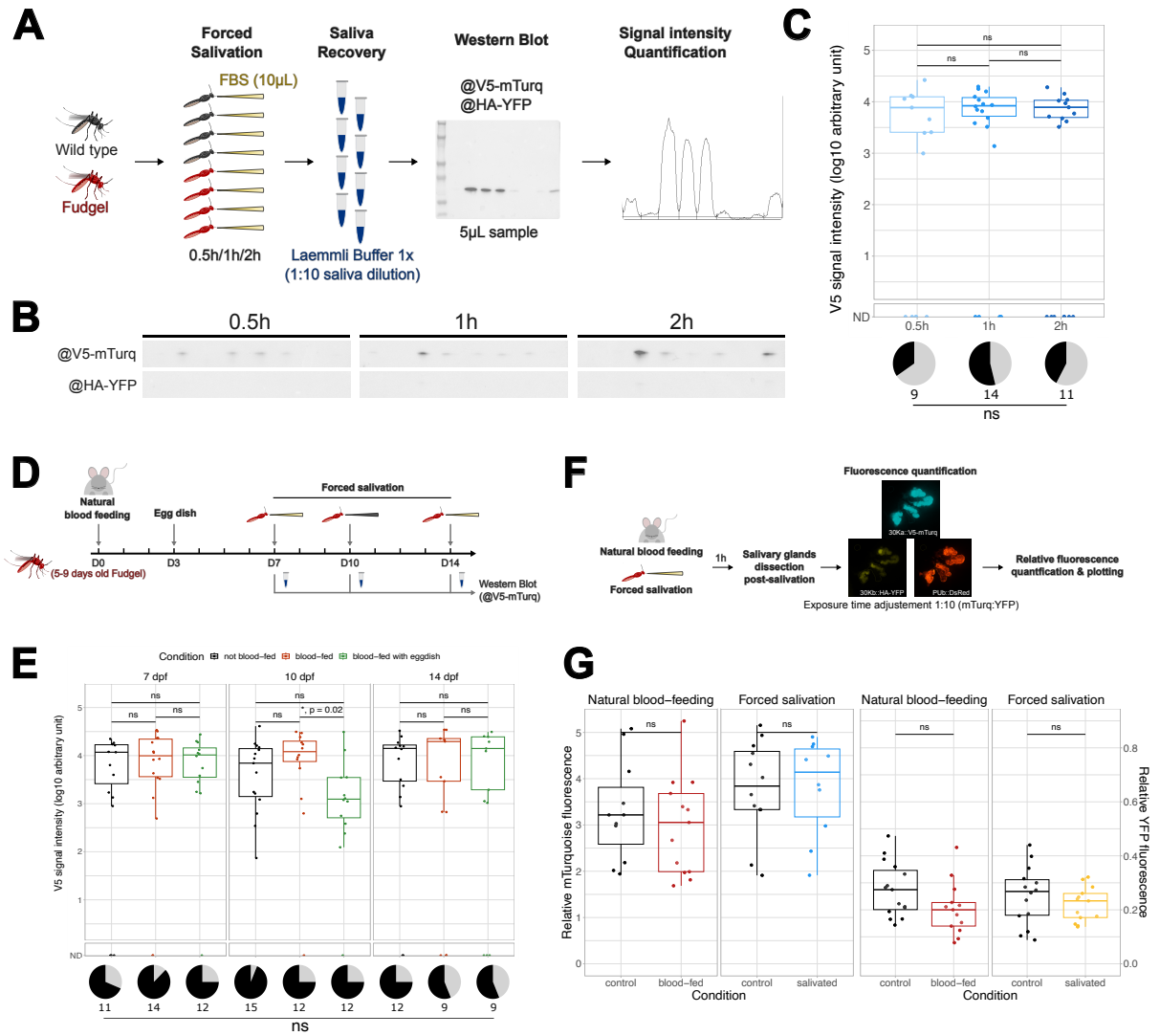

Figure 2- Fluorescence marker detection can be used as a reporter for salivation performance

A) Experimental design for detection and quantification of marker expression after forced salivation. **B**) Western Blot signal for V5 and HA in individual saliva samples of Fudgel mosquitoes after 0.5h, 1h or 2h of forced salivation. **C**) V5 signal intensity in individual saliva samples of Fudgel mosquitoes at different times (n = 20 saliva samples per time point) (log10 scale). **D**) Experimental design for testing the effect of different physiological states on salivation. **E**) V5 signal intensity in individual saliva samples of Fudgel mosquitoes in different physiological states after 1h of forced salivation (n = 16 per condition) (log10 scale). **F**) Experimental design for testing the effect of salivation on salivary glands. **G**) mTurq and YFP fluorescence intensity relative to dsRED (CTCF(marker/dsRED)) in individual salivary glands of Fudgel mosquitoes 1h after blood-feeding on mice or forced salivation. Exposure time was 10-fold higher for YFP compared to mTurq. Comparison of signal intensity: Kruskall-Wallis test, threshold 0.05. Comparison of prevalence of salivation: Fisher's exact test, threshold 0.05.

186 The interaction between mosquito saliva proteins and skin cells after biting has been thoroughly studied
187 *in vitro* using mammalian cell lines or recombinant proteins[35–37]. However, *in vivo* analyses are harder
188 to perform due to the lack of tools to precisely identify and isolate mosquito biting sites and track saliva
189 factors. Tracking mosquito salivation on a mammalian host after biting would allow precise monitoring
190 of viral replication sites and local immune responses. Since we observed active release of mTurq during
191 forced salivation on a Petri dish (**Supplementary video 1**), we next tested whether the fluorescent
192 markers could be detected directly in human skin explants exposed to mosquitoes (**Figure 3a**). When
193 allowed, mosquitoes actively probed the skin explants but could not feed as coagulation already
194 occurred in the cutaneous blood vessels (**Figure 3b**). On a fluorescent microscope, we were able to
195 visualize mosquito bite sites via tracking mTurq and YFP fluorescent markers immediately after probing
196 (**Figure 3c**). Of note, dsRED expressed under a ubiquitous promoter and lacking a signal peptide was
197 not detected at the bite site (**Figure 3c**). This suggests specific secretion and release of the fluorescent
198 markers expressed under the control of the bidirectional 30K promoter during probing on the skin
199 explants. Thus, our mosquito line allows efficient tracking of bite sites and the release of saliva factors
200 in the skin.
201

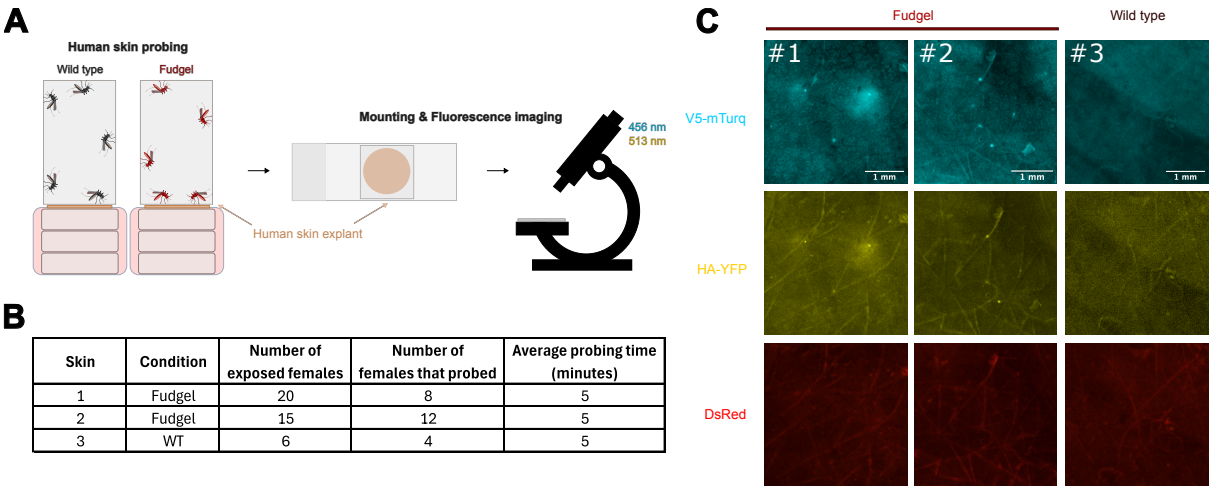

Skin	Condition	Number of exposed females	Number of females that probed	Average probing time (minutes)
1	Fudgel	20	8	5
2	Fudgel	15	12	5
3	WT	6	4	5

202
203 **Figure 3- Fluorescent markers allow tracking of probing sites on human skin**
204 **A**) Experimental design for the analysis of probing on human skin explants. **B**) Mosquito exposure
205 condition and time for each skin explant. **C**) Detection of mTurq and YFP fluorescence at probing foci
206 on each tested human skin explant directly after probing. Exposure time was 10-fold higher for YFP
207 compared to mTurq.
208
209 **Virus transmission and mosquito salivation**
210
211 Mosquito-borne viruses are transmitted by mosquitoes through biting and virus detection in forced
212 salivation assays is often used as a measure of transmission[25,26]. However, in these assays, quantifying
213 the release of saliva factors is rarely performed due to the lack of experimental tools. Mosquito
214 engorgement with buffer or measurements of the volume of release liquid in oil-filled capillary tubes
215 have both been used as a proxy for salivation[22,23]. To overcome these limitations, we used the Fudgel
216 line to investigate the connection between salivation and virus transmission (**Figure 4a**). In the following

217 assays, mosquitoes were infected with ZIKV by intrathoracic injection to guarantee homogenous
218 systemic dissemination, since we wanted to analyze salivary gland infection and virus presence in the
219 saliva. Viral loads in infected Fudgel mosquitoes carcasses were not significantly different from non-
220 transgenic controls showing that the transgene does not affect infection (**Figure 4b**). Using a forced
221 salivation protocol, we observed that salivation performance was significantly reduced in ZIKV infected
222 Fudgel mosquitoes, which displayed a lower proportion of individuals with detectable marker in the
223 saliva (26 out of 40) compared to non-infected mosquitoes (16 out of 16) (**Figure 4c).** mTurq levels in
224 infected individuals were not significantly different from non-infected controls, suggesting that the effect
225 observed in response to ZIKV infection is due to a decrease in the release of saliva factors and not in
226 the expression of the reporter (**Figure 4d**). We next measured the presence of infectious virus in the
227 saliva samples from the same individual mosquitoes. Out of 40 tested saliva samples from infected
228 Fudgel mosquitoes, 9 had a cytopathic effect on cells (shown in green on **Figure 4c**). In these samples,
229 we observed no correlation between salivation performance and detection of the virus (**Figure 4c**). Of
230 note, two ZIKV-positive samples had no detectable saliva (**Figure 4c**). These data were obtained in two
231 independent experiments with similar results (**Supplementary figure 6a,b** and **Supplementary table**
232 **6,7**). To verify if the effect of virus infection on salivation was restricted to ZIKV, we next analyzed
233 mosquitoes infected with CHIKV by intrathoracic injection. Fudgel mosquitoes showed similar CHIKV
234 levels compared to controls showing no effects of the transgene on viral infection (**Figure 4e**). Similar
235 to ZIKV, we observed a decrease in salivation performance in CHIKV infected mosquitoes with a
236 decreased proportion of salivating individuals (38 out of 54) compared to non-infected controls (19 out
237 of 20), and an additional significant decrease in the amount of detected saliva factors in the 38 saliva
238 samples that had detectable saliva (**Figure 4f**). Out of 54 samples, 5 were infectious on mammalian
239 cells (shown in purple on **Figure 4f**) and again we observed no correlation between virus detection and
240 the amount of detected saliva factors. No difference between levels of mTurq marker in CHIKV infected
241 mosquitoes compared to controls were observed, suggesting a specific effect on the release of saliva
242 factors and not of the production of the marker in the salivary gland (**Figure 4g**). These results were
243 obtained from three independent experiments with very similar results (**Supplementary figure 6c** and
244 **Supplementary table 6,7**). Together, these results suggest that virus infection decreases the release
245 of saliva factors by infected salivary glands. In addition, our data indicate no correlation between the
246 release of saliva factors and infectious viruses.
247

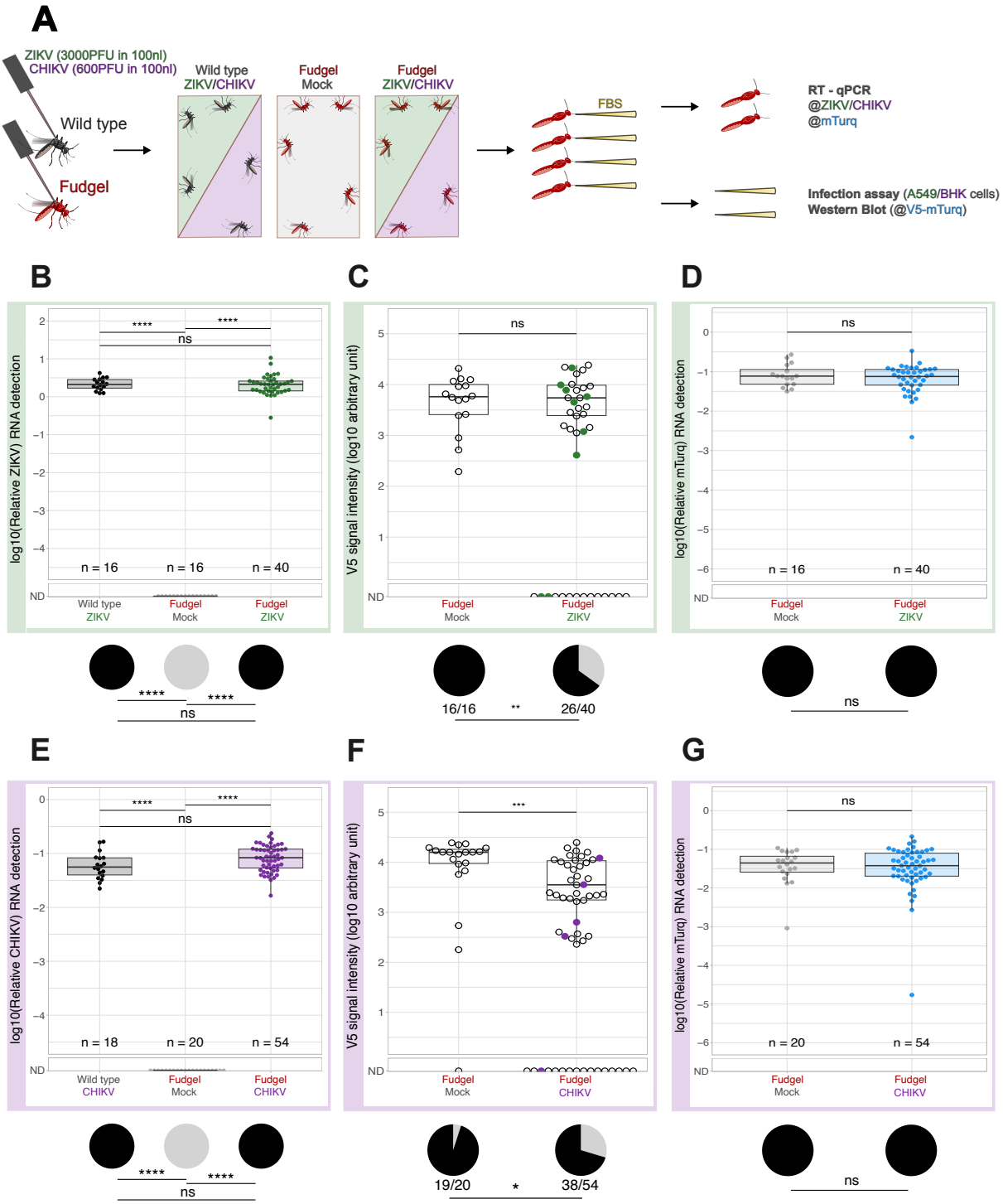

Figure 4- Infection with ZIKV or CHIKV significantly decreases salivation performance in mosquitoes

A) Experimental design for the analysis of salivation in mosquitoes infected with ZIKV or CHIKV. **B**) Detection of ZIKV by RT-qPCR in mosquitoes at 14 days post infection. **C**) V5 signal intensity in individual samples of control or ZIKV-infected mosquitoes. Saliva samples associated with the presence of infectious virus are marked in green. **D**) Detection of V5-mTurq expression by RT-qPCR in control and ZIKV-infected mosquitoes. **E**) Detection of CHIKV by RT-qPCR in mosquitoes at 9 days post infection. **F**) V5 signal intensity in individual samples of control or CHIKV-infected mosquitoes. Saliva

258 samples associated with the presence of infectious virus are marked in purple. **G**) Detection of V5-
259 mTurq expression by RT-qPCR in control and CHIKV-infected mosquitoes. Comparison of viral loads
260 in carcasses, V5 signal intensity and V5-mTurq levels in carcasses: Kruskall-Wallis test, threshold 0.05.
261 Comparison of prevalences: Fisher's exact test, threshold 0.05.
262
263 **Discussion**
264
265 In this study, we developed a transgenic mosquito line expressing fluorescent markers that function as
266 reporters for salivation. This line allowed us to study basic aspects of the physiology of salivation. We
267 first analyzed the evolution of salivation behavior through a gonotrophic cycle, e. g. from eggs
268 development to their oviposition. We could highlight a transient decrease in salivation performance at
269 10 dpf for mosquitoes completing of a full cycle, which was observed neither in mosquitoes that were
270 not allowed to lay eggs after feeding nor in those who did not blood feed. Previous studies suggest
271 hormonal variations through the reproduction cycle of female mosquitoes which would be associated
272 with modifications in host seeking and blood feeding behaviors[34]. The observed transient decrease in
273 salivation performance goes along with a decreased host seeking behavior associated with the start of
274 a new gonotrophic cycle. This phenomenon would need to be further characterized, and our tool shows
275 great potential to match this purpose. We also measured the effect of natural blood-feeding or forced
276 salivation on salivary glands purging, without detecting any significant difference in saliva content
277 compared to not blood-fed or non-salivating controls. Moreover, this tool allowed us to precisely
278 visualize mosquito probing sites on human skin explants, highlighting its potential use for *in vivo*
279 transmission studies. This could be an important tool to examine skin cells response to saliva
280 components specifically at the biting site, in both non-infected and virus-infected settings.
281
282 In the context of infection, we showed that both ZIKV or CHIKV decreased mosquito salivation, affecting
283 both the proportion of mosquitoes that secreted detectable levels of saliva factors as well as the amount
284 of released saliva. Since these viruses did not affect the expression of markers in the salivary gland,
285 our results suggest a specific effect of these viruses on the secretion of saliva factors. Interestingly,
286 some changes to infected acinar cells were observed in salivary glands by electron microscopy[11], which
287 could indicate damage and explain why there is an impact on salivation. Our results also showed that
288 the levels of saliva factors do not correlate with release of the virus in the saliva. In agreement with this
289 disconnect, electron microscopy studies of CHIKV infected salivary glands suggested that viral particles
290 segregate in separate vesicles from the saliva factors in acinar cells[11]. Independent release of virus and
291 saliva proteins during salivation could explain the observed absence of correlation between salivation
292 performance and virus transmission. This is a shift from the common assumption that viral transmission
293 efficiency correlates with the quantity of released saliva factors. Of note, genetic depletion of salivary
294 glands or microsurgery removal of the salivary duct caused a reduction in salivation and increased
295 probing behavior in *Anopheles* mosquitoes[38,39]. Thus, reduced release of saliva factors in virus-infected
296 mosquitoes should lead to an increase in probing and biting behavior. Accordingly, previous studies
297 have shown that dengue-infected mosquitoes have increased biting behavior compared to uninfected

298 controls [40]. This makes sense in light of data showing that successive short probing events resulted in
299 multiple deposition of the virus[40]. Damaging the salivary glands could thus be a strategy used by the
300 virus to reduce salivation and increase the probing behavior to enhance viral transmission. Further
301 studies are required to clarify how the infection affects salivary glands and salivation. A similar situation
302 might occur in *Anopheles* mosquitoes, where there are significant changes in salivary glands
303 morphology and loss of integrity upon *Plasmodium* infection[41]. The authors observed an alteration of
304 saliva composition with a decrease of detected proteins and diffusion of saliva proteins in the mosquito
305 hemolymph. At the same time, no difference was observed in the volume of saliva released from
306 *Plasmodium*-infected mosquitoes although they seemed to probe for longer times[38,41]. Overall, these
307 data suggest that increased probing, especially without reduction of the volume of liquid released, would
308 serve to increase transmission of pathogens by the mosquito bite. Our results may also help explain
309 recent epidemiological observations that low levels of circulating antibodies against the D7 *Aedes*
310 salivary protein correlate with a higher infection burden of DENV in human populations living in *Aedes*
311 endemic populations[42]. These results align with the hypothesis that viral infection reduces the secretion
312 of saliva factors by the mosquito.
313
314 Finally, beyond the effect of infection on salivation and transmission, expression and secretion of saliva
315 factors can be impacted by the virus. Some salivary gland genes such as 30Ka have increased
316 expression at 5 and 14 days post DENV infection[43,44]. Similarly, the SAAG-4 protein encoded by the
317 30Ka gene is up-regulated 5 days after CHIKV infection in the salivary glands[45]. In contrast, SAAG-4 is
318 down-regulated in the salivary glands at 3 days and in the saliva at 10 days after DENV infection[45,46].
319
320 All these observations highlight a complex, multi-layered interaction between the virus, salivary glands
321 and secreted saliva factors. We hope that the Fudgel line will help gain valuable insights on the
322 physiology of salivation with or without viral infection, from saliva production to its release.
323
324 **Material and methods**
325
326 **Cloning, transgenesis and Fudgel line establishment**
327 Sequences of the 30K bidirectional promoter and associated signal peptides were recovered from the
328 AaegL5 LVP_AGWG reference genome on the VectorBase database
329 (https://vectorbase.org/vectorbase/app) and synthesized as a gBlock gene fragment (IDT). The gBlock
330 sequence was cloned using the NEBuilder® HiFi DNA Assembly Cloning kit (ref E5520S) in a pSKB-
331 plasmid (Addgene #62540), previously linearized by PCR amplification using the ThermoFisher
332 Scientific DreamTaq DNA polymerase (ref EP0701) (primers in **Supplementary table 8**). The
333 sequences for epitope-tagged fluorescent markers were amplified from lab stock plasmids by PCR
334 using the ThermoFisher Scientific Phusion High-Fidelity DNA polymerase (ref F530S) (primers in
335 **Supplementary table 8**). A backbone plasmid containing the pUb::dsRED::SV40 sequence was
336 digested using BamHI and SmaI restriction enzymes (Anza) The final construct was cloned using
337 NEBuilder® HiFi DNA Assembly Cloning kit (ref E5520S).

338
339 This plasmid was injected at a concentration of 300 ng/µL in mosquito eggs with 100 ng/µL of a helper,
340 codon-optimized piggyBac transposase-expressing plasmid[47] (available on request) in 0.5x PBS as
341 follows: mosquito females of the Bangkok strain were blood-fed 4 days prior to injection and allowed to
342 lay eggs. One hour-old eggs were aligned along wet paper on a microscope slide and injected in their
343 posterior pole using a Nikon ECLIPSE TE2000-S inverted microscope, Eppendorf Femtojet 4x micro-
344 injector and Eppendorf TransferMan NK2 control panel. Injected G0 larvae were screened and
345 individuals displaying transient dsRED fluorescence expression were backcrossed to wild-type
346 Bangkok mosquitoes. From their G1 progeny, dsRED-positive individuals were selected under a
347 fluorescent binocular microscope (Nikon SMZ18 microscope, sola light engine Lumencor® laser),
348 backcrossed, and progeny was again individually backcrossed. In G3, populations showing 50%
349 inheritance of the transgene were selected, suggestive of a single transgene insertion. Positive G3
350 mosquitoes of a given population were self-crossed. Homozygous – single insertion – G4 mosquitoes
351 were sorted based on fluorescence intensity using the COPAS instrument[48] to generate the Fudgel line
352 (**Supplementary figure 1b,c**). Experiments were carried on using mosquitoes from G5 on.
353
354 **Transgene insertion mapping by inverse PCR**
355 Genomic Fudgel DNA was extracted from five homozygous male pupae using the Monarch DNA
356 purification kit (ref T3010S/L) and quantified with Nanodrop. Extracted DNA (1µg) was digested with
357 AarI, AgeI, ApeI, SacII and XhoI restriction enzymes (FastDigest — Thermo Scientific) for 1 hour at
358 37°C and enzymes were inactivated for 10 minutes at 80°C. The digested DNA was treated with T4
359 DNA ligase (50 Units of enzyme for a 500µL reaction, Thermo Scientific ref EL0011) overnight at room
360 temperature. DNA was then purified using the Macherey-Nagel NucleoSpin Gel and PCR Clean-up kit
361 (ref 11992242) and amplified by nested-PCR using the ThermoFisher Scientific DreamTaq DNA
362 polymerase (ref EP0701). Primers for both PCR were designed to amplify the 3' region of the transgene
363 (**Supplementary table 8**). The remaining 15µL of the PCR were Sanger sequenced (GATC Biotech,
364 Eurofins) and blasted on the AaegL5 LVP_AGWG reference genome on VectorBase. This alignment
365 returned 1 hit on chromosome 3 (AaegL5_3:251028673:f). Deduced flanking genomic sequences were
366 confirmed on both the 5' and 3' sides of the piggyBac element by PCR amplification using the
367 ThermoFisher Scientific Dreamtaq Green MasterMix (ref K1081) (primers in **Supplementary table 8**)
368 and sequenced (GATC Biotech, Eurofins).
369
370 **Salivation protocol optimization**
371 Fudgel female mosquitoes were starved 24h prior to experiment. The day of the salivation, mosquitoes
372 were anesthetized with CO_2 and kept on ice. Legs and wings were removed, and proboscis inserted in
373 tips containing 10µL of FBS (Fetal Bovine Serum). Mosquitoes were left to salivate either 30 minutes,
374 1 hour or 2 hours, then saliva samples were collected. Each mosquito was considered a biological
375 replicate.
376
377 **Marker detection and quantification by Western Blot**

378 Saliva samples were diluted 1:10 in 1x Laemmli Buffer and heated for 20 minutes at 95°C. Heating
379 process was repeated depending on experimental set up. Samples were then resolved on Mini-
380 PROTEAN TGX Stain-Free Precast Gel 4-15% (Bio Rad ref #4568086) and transferred to a
381 Nitrocellulose membrane (Trans-Blot Turbo Transfer Pack Bio Rad ref #1704158). Membranes were
382 blocked with 5% BSA (Albumine, from bovine serum SIGMA ref A3059) in PBS-Tween 0.1% solutions
383 and treated with either @HA-HRP (Roche ref 12013819001) or @V5-HRP (Invitrogen ref 46-0708)
384 antibodies 1:5000 in 1.5% BSA in PBS-Tween 0.1%. Membranes were incubated in the antibody
385 solution under agitation either 1 hour at room temperature or overnight at 4°C, rinsed in PBS-Tween
386 0.1%. Protein signal was revealed with ECL Select (Cytiva ref GERPN2235) using a ChemiDoc imaging
387 system (BioRad). Membranes were revealed using the Chemidoc Imaging System from Bio Rad.
388 Western Blot images were treated with the ImageJ software. Rectangular selection of signal from all
389 samples of the membrane constitutes a "lane": *Analyze/Gels/Select First Lane*. Bands intensity was
390 then plotted: *Analyze/Gels/Plot Lanes*, and relative band intensities recovered with the *Wand* tool.
391 Intensity values were then recorded, plotted on a log10 scale, and processed with the RStudio software
392 with the *ggplot2* and associated packages[49,50]. Saliva tag signal levels between conditions were
393 compared using a Kruskal-Wallis test.
394
395 **Fluorescent marker imaging**
396 Mosquitoes were anaesthetized with CO_2 and kept on ice. Whole body and proboscis images were
397 acquired on a fluorescent binocular microscope (Nikon SMZ18 microscope, sola light engine
398 Lumencor® laser) (**Figure 1d,f**). For salivary gland acquisitions (**Figure 1e**), dissections were
399 performed in PBS under a fluorescence microscope and the salivary glands were fixed in PFA 4% for
400 1h40 at room temperature (RT). Samples were then permeabilized in PBS-T (0.2% Triton 100x, 1%
401 BSA) for 45 minutes at RT and incubated with DAPI (1:1000 in PBS-T) for 10 minutes at RT. Salivary
402 glands were rinsed 3 x 10 minutes in PBS-T and mounted on slides using VECTASHIELD Antifade
403 mounting medium (Vectorlabs, ref H-1000). Acquisitions were performed on an epifluorescence
404 microscope Axioskop 2 (Zeiss). For confocal image acquisitions (**Supplementary figure 1d**) salivary
405 glands and mosquito heads were dissected in PBS under a fluorescent stereoscope. Fresh tissues
406 were mounted in VECTASHIELD mounting medium and confocal 10x Z stack acquisitions were
407 performed using a spinning disk inverted microscope (Zeiss, Axio Observer Z1). Stack images were
408 merged using the "Extended Depth of Field" plugin in ImageJ [51]: Direct Method, Expert Mode, EDF
409 "Complex Wavelets". For proboscis, acquired images were despeckled (*Process/Noise/Despeckle*)
410 prior to merging to avoid signal loss.
411
412 **Salivation recording**
413 Mosquitoes were anaesthetized with CO_2 and kept on ice. Legs and wings were removed, and
414 proboscis put in FBS drops. Mosquitoes were left to salivate at room temperature for 1 hour. Mosquitoes
415 and droplets were then observed under a fluorescent microscope (Zeiss SteREO Discovery.V8
416 microscope, X-Cite Xylis Excelitas Technologies laser) to witness salivation and for video recording
417 (**Supplementary video 1**).

418
419 **Physiological state and salivation**
420 5 to 8 days old Fudgel mosquitoes were blood-fed or not on mice anaesthetized with a solution of NaCl
421 0.9%, Rompun 2%, Zoletil 50. 3 days post-feeding fed females were given or not an egg dish to lay
422 their eggs. Egg dishes were removed after 3 days. Of note, blood-fed females without the egg dishes
423 had minor residual oviposition on the sugar pads. At day 7, day 10 and day 14 post-feeding, mosquitoes
424 were anaesthetized with CO_2, legs and wings removed, and females from the different feeding
425 conditions were put to salivate in 10µL FBS for 1 hour. 18 hours prior to salivation, mosquitoes were
426 starved by replacing sugar with water only. Not blood-fed Bangkok females of the same age were used
427 as negative control. Individual saliva samples were collected and diluted 1:10 in Laemmli 1x. The
428 samples were then analyzed by Western Blot with @V5-HRP antibody treatment.
429
430 **Salivary gland fluorescence intensity after natural blood feeding or forced salivation**
431 For blood feeding, mosquitoes were starved the prior day. Half of mosquitoes were allowed to fully
432 engorge on a mouse anaesthetized with a solution of NaCl 0.9%, Rompun 2%, Zoletil 50. For forced
433 salivation, mosquitoes were anaesthetized with CO_2 and kept on ice. Legs and wings were removed,
434 and half of them were put to salivate in 10µL FBS for 1 hour at RT. The salivary glands of control
435 mosquitoes, blood-fed mosquitoes, and mosquitoes that salivated were dissected under a fluorescent
436 binocular microscope (Nikon SMZ18 microscope, sola light engine Lumencor® laser). For each
437 condition of each replicate, between 6 and 8 salivary glands were dissected and analyzed. Pictures
438 were acquired with a fluorescent binocular microscope (Nikon SMZ18 microscope, sola light engine
439 Lumencor® laser). Fluorescence intensity quantification was done using ImageJ. For mTurquoise, YFP
440 and dsRED, we calculated the Corrected Total Cell Fluorescence (CTCF):
441
442 $$CTCF_{marker} = fluorescence\ intensity - (Area\ x\ Background\ mean)$$
443
444 $$\rho CTCF = \frac{CTCF_{marker}}{CTCF_{dsRED}}$$
445
446 Fluorescence intensity was normalized using ρCTCF, defined as the ratio between the CTCF value of
447 the salivation marker – either mTurq or YFP – and the CTCF of the dsRED transgenesis reporter.
448 ρCTCF for each marker of individual salivary glands are plotted using the *ggplot2* and associated
449 packages[49,50] on RStudio.
450
451 **Saliva detection in human skin explants**
452 Human skin explants were recovered from anonymized patients who underwent abdominal reduction
453 (St Anne Clinic, Strasbourg), with written informed consent and institutional review board approval, in
454 agreement with the Helsinki Declaration and French legislation. At reception, skin surfaces were wiped
455 successively with 70% ethanol, antiseptic solution (Dakin®) and phosphate buffer saline (Corning).
456 Superficial layers of the skins (200µm thickness) were harvested using a dermatome blade and

457 incubated in complete DMEM medium (10% fetal calf serum, 0.1mg/mL streptomycin and 10µg/mL
458 gentamycin) overnight at 37°C, 5% CO_2. The night prior to experiment, 5 female mosquitoes were put
459 in drosophila culture tubes and starved until the experiment. Human skins explants were put in contact
460 with starved mosquitoes and each batch of mosquitoes was allowed to probe for 10 minutes. Different
461 skin samples were then recovered, placed in 1x PBS and immediately observed under a fluorescent
462 binocular microscope (Nikon SMZ18 microscope, sola light engine Lumencor® laser). Pictures were
463 acquired using a Nikon DS-Ri2 camera.
464
465 **ZIKV and CHIKV infections**
466 One week old Bangkok and Fudgel female mosquitoes were transferred to a Biosafety Level 3
467 laboratory, anesthetized with CO_2 and kept on ice. Injections were performed using a Nanoject III micro-
468 injector (Dummond Scientific Company Cat. 3-000-207). Both ZIKV and CHIKV were tested in
469 independent experiments, in duplicates and triplicates respectively. Bangkok females were injected with
470 either 3000 PFU of ZIKV or 600 PFU of CHIKV in 100nL. Fudgel females were injected with either Mock
471 solution (virus growth medium: Gibco Leibovitz's L-15 Medium), or with 100nL of virus. They were left
472 to recover and incubate. Forced salivations were performed at either 14 days post-injection (dpi) or 9
473 dpi respectively for ZIKV and CHIKV.
474
475 Mosquitoes were starved (deprived of sugar and water) the day before the experiment and anesthetized
476 with triethylamine (N,N-Diethylethanamine, SIGMA-Aldrich ref T0886). Legs and wings were removed,
477 and proboscis inserted in tips filled with 10µL FBS. Mosquitoes were left to salivate for 1 hour at RT.
478 Saliva samples and carcasses were then recovered for analysis. ZIKV and CHIKV RNA levels in
479 carcasses were measured by RT-qPCR (primers in **Supplementary table 8**). RNA was extracted using
480 the Mag-Bind Total RNA kit (Omega bio-tek ref M6731-01) at half-volumes and the KingFisher Apex
481 machinery (Thermo Scientific). Reverse transcription was performed using RevertAid H Minus enzyme
482 (Thermo Scientific ref EP0452) with random hexamers, and qPCR with PowerSYBR Green PCR Master
483 Mix (Applied Biosystems ref 4367659) and the reaction ran on Quant Studio 5 machinery (Applied
484 Biosystems). Results were processed using the apps.thermofisher.com platform and plotted with
485 *ggplot2* and associated packages[49,50] on RStudio. To quantify salivation levels, 2µL of each saliva
486 sample were mixed with 18µL of Laemmli 1x (1:10) and analyzed by Western Blot with @V5-HRP
487 antibody. Signal intensity was quantified using ImageJ and plotted with *ggplot2* and associated
488 packages[49,50] on RStudio.
489
490 Of the remaining saliva samples from CHIKV experiments, 5µL were used to perform an infection assay
491 on BHK cells. Cells were previously grown in DMEM medium (10% FBS, 1% Penicillin/Streptomycin
492 (P/S)) at 37°C, 5% CO2. 24h prior to infection, cells were diluted to 10^{-4} cells/100µL in DMEM medium
493 (5% FBS, 1% P/S) and sampled in 96 well plates. Saliva samples were diluted in series in DMEM
494 medium (0% FBS, 2% antibiotic-antimycotic, 1% P/S) and put on cells, from 10^{-2} to 10^{-7} dilution,
495 100µL/well, each dilution in quadruplicates. Viral stock dilutions from 10^{-4} to 10^{-9} in quadruplicates were
496 used as a positive control for cells infection. Non-infected saliva samples were used as negative

controls. Cells were left to incubate with the virus at 37°C, 5% CO_2. Cytopathic effect was measured from 3dpi to 7dpi. For ZIKV saliva samples, 2µL of each individual saliva samples were used to infect interferon-deficient A549 cells. Cells were grown and prepared as detailed for BHK cells. Saliva samples were diluted in 100µL of DMEM medium (0% FBS, 2% antibiotic-antimycotic, 1% P/S) and put on cells (50x dilution). Each saliva sample was used on one single cell well. Viral stock dilutions from 10^{-4} to 10^{-9} in triplicates were used as a positive control for cells infection. Non-infected saliva samples were used as negative controls. Cells were left to incubate with the virus at 37°C, 5% CO_2. Cytopathic effect was measured from 3dpi to 7dpi.

Acknowledgements

We thank members of the Mosquito Immune Response team for comments and discussions and staff at UPR9022 and U1257 for technical support, and especially Marcela Celis for maintenance of mosquito lines. This work was supported by grants from Conselho Nacional de Desenvolvimento Científico e Tecnológico (CNPq) to J.T.M.; Fundação de Amparo a Pesquisa do Estado de Minas Gerais (FAPEMIG), Instituto Nacional de Ciência e Tecnologia de Vacinas (INCTV) to J.T.M.; Fonds régional de coopération pour la recherche FRCT2020 Région Grand-Est – ViroMod to J.T.M. and C. M.; Institute for Advanced Studies of the University of Strasbourg (USIAS fellowship 2019) to J.T.M.; Human Frontiers Since Program (RGP018/2023) to J.T.M.; Agence Nationale de la Recherche ANR-21-CE12-0024 and ANR-24-CE15-4470 to J.T.M. and , ANR-19-CE35-0007 to E.M. and J. T. M.. This study was financed in part by the Coordenação de Aperfeiçoamento de Pessoal de Nível Superior — Brasil (CAPES) — Finance Code 001 to J.T.M. This work of the Interdisciplinary Thematic Institute IMCBio, as part of the ITI 2021-2028 program of the University of Strasbourg, CNRS and Inserm, was supported by IdEx Unistra (ANR-10-IDEX-0002), by SFRI-STRAT'US project (ANR 20-SFRI-0012), and EUR IMCBio (IMCBio ANR-17-EURE-0023) under the framework of the French Investments for the Future Program to J.T.M.. L.S. was supported by fellowships from IMCBio and FRM (Programme Fin de Thèse FDT2024040 18199). The funders had no role in study design, data collection and analysis, decision to publish, or preparation of the manuscript.

Author contributions

L.S., M.B. and J.T.M. designed the project. L.S., M.B., B.V., T.H.J.F.L., E.M. and F.A. performed experiments. L.S. and J.T.M. analysed the data. L.S. and J.T.M. wrote the paper. All authors discussed the results and edited the manuscript.

Competing interests

The authors declare no competing interests.

533 **References**

534

535 1. Liu-Helmersson, J., Brännström, Å., Sewe, M. O., Semenza, J. C. & Rocklöv, J. Estimating Past,
536 Present, and Future Trends in the Global Distribution and Abundance of the Arbovirus Vector
537 Aedes aegypti Under Climate Change Scenarios. *Front. Public Health* **7**, 148 (2019).
538 2. Messina, J. P. *et al.* The current and future global distribution and population at risk of dengue. *Nat.*
539 *Microbiol. 2019 49* **4**, 1508–1515 (2019).
540 3. Crawford, J. E. *et al.* Population genomics reveals that an anthropophilic population of Aedes aegypti
541 mosquitoes in West Africa recently gave rise to American and Asian populations of this major
542 disease vector. *BMC Biol.* **15**, 16 (2017).
543 4. Rose, N. H. *et al.* Dating the origin and spread of specialization on human hosts in Aedes aegypti
544 mosquitoes. *eLife* **12**, e83524 (2023).
545 5. Atoni, E. *et al.* The discovery and global distribution of novel mosquito-associated viruses in the last
546 decade (2007-2017). *Rev. Med. Virol.* **29**, e2079 (2019).
547 6. Bhatt, S. *et al.* The global distribution and burden of dengue. *Nat. 2013 4967446* **496**, 504–507
548 (2013).
549 7. Grabenstein, J. D. & Tomar, A. S. Global geotemporal distribution of chikungunya disease, 2011–
550 2022. *Travel Med. Infect. Dis.* **54**, 102603 (2023).
551 8. Kraemer, M. U. *et al.* The global distribution of the arbovirus vectors Aedes aegypti and Ae.
552 albopictus. *eLife* **4**, e08347 (2015).
553 9. Wu, P., Yu, X., Wang, P. & Cheng, G. Arbovirus lifecycle in mosquito: acquisition, propagation and
554 transmission. *Expert Rev. Mol. Med.* **21**, e1 (2019).
555 10. Raquin, V. & Lambrechts, L. Dengue virus replicates and accumulates in *Aedes aegypti* salivary
556 glands. *Virology* **507**, 75–81 (2017).
557 11. Vega-Rúa, A., Schmitt, C., Bonne, I., Krijnse Locker, J. & Failloux, A.-B. Chikungunya Virus
558 Replication in Salivary Glands of the Mosquito Aedes albopictus. *Viruses* **7**, 5902–5907 (2015).
559 12. Visser, I., Koenraadt, C. J. M., Koopmans, M. P. G. & Rockx, B. The significance of mosquito saliva
560 in arbovirus transmission and pathogenesis in the vertebrate host. *One Health* **16**, 100506 (2023).
561 13. Arnoldi, I. *et al.* A salivary factor binds a cuticular protein and modulates biting by inducing
562 morphological changes in the mosquito labrum. *Curr. Biol.* **32**, 3493-3504.e11 (2022).

563 14. Sun, P. *et al.* A mosquito salivary protein promotes flavivirus transmission by activation of
564 autophagy. *Nat. Commun.* **11**, 1–15 (2020).
565 15. Lefteri, D. A. *et al.* Mosquito saliva enhances virus infection through sialokinin-dependent vascular
566 leakage. *Proc. Natl. Acad. Sci.* **119**, e2114309119 (2022).
567 16. Conway, M. J. *et al.* Aedes aegypti D7 Saliva Protein Inhibits Dengue Virus Infection. *PLoS Negl.*
568 *Trop. Dis.* **10**, e0004941 (2016).
569 17. McCracken, M. *et al.* Aedes aegypti salivary protein "aegyptin" co-inoculation modulates dengue
570 virus infection in the vertebrate host. *Virology* **0**, 133–139 (2014).
571 18. McCracken, M. K., Christofferson, R. C., Chisenhall, D. M. & Mores, C. N. Analysis of Early Dengue
572 Virus Infection in Mice as Modulated by Aedes aegypti Probing. *J. Virol.* **88**, 1881–1889 (2014).
573 19. Edwards, J. F., Higgs, S. & Beaty, B. J. Mosquito feeding-induced enhancement of Cache Valley
574 Virus (Bunyaviridae) infection in mice. *J. Med. Entomol.* **35**, 261–265 (1998).
575 20. Conway, M. J. *et al.* Mosquito Saliva Serine Protease Enhances Dissemination of Dengue Virus
576 into the Mammalian Host. *J. Virol.* **88**, 164–175 (2014).
577 21. Schmid, M. A. *et al.* Mosquito Saliva Increases Endothelial Permeability in the Skin, Immune Cell
578 Migration, and Dengue Pathogenesis during Antibody-Dependent Enhancement. *PLOS Pathog.*
579 **12**, e1005676 (2016).
580 22. Novak, M. G., Ribeiro, J. M. C. & Hildebrand, J. G. 5-Hydroxytryptamine in the Salivary glands Of
581 Adult Female Aedes Aegypti and its Role in Regulation of Salivation. *J. Exp. Biol.* **198**, 167–174
582 (1995).
583 23. Ribeiro, J. M. C. & Valenzuela, J. G. The salivary purine nucleosidase of the mosquito, *Aedes*
584 *aegypti*. *Insect Biochem. Mol. Biol.* **33**, 13–22 (2003).
585 24. Heitmann, A. *et al.* Forced Salivation As a Method to Analyze Vector Competence of Mosquitoes.
586 *J. Vis. Exp. JoVE* 57980 (2018) doi:10.3791/57980.
587 25. Miller, M. R. *et al.* Characterizing and Quantifying Arbovirus Transmission by Aedes aegypti Using
588 Forced Salivation and Analysis of Bloodmeals. *Insects* **12**, 304 (2021).
589 26. Gloria-Soria, A., Brackney, D. E. & Armstrong, P. M. Saliva collection via capillary method may
590 underestimate arboviral transmission by mosquitoes. *Parasit. Vectors* **15**, 103 (2022).
591 27. Juhn, J. *et al.* Spatial mapping of gene expression in the salivary glands of the dengue vector
592 mosquito, Aedes aegypti. *Parasit. Vectors* **4**, 1 (2011).

593 28. Ribeiro, J. M. *et al.* An annotated catalogue of salivary gland transcripts in the adult female
594 mosquito, Ædes ægypti*. *BMC Genomics* **8**, 6 (2007).
595 29. Goldman, O. V. *et al.* Mosquito Cell Atlas: A single-nucleus transcriptomic atlas of the adult Aedes
596 aegypti mosquito. 2025.02.25.639765 Preprint at https://doi.org/10.1101/2025.02.25.639765
597 (2025).
598 30. Boppana, V. D., Thangamani, S., Adler, A. J. & Wikel, S. K. SAAG-4 is a Novel Mosquito Salivary
599 Protein that Programs Host CD4+ T Cells to Express IL-41. *Parasite Immunol.* **31**, 287–295 (2009).
600 31. Calvo, E. *et al.* Aegyptin, a Novel Mosquito Salivary Gland Protein Specifically Binds to Collagen
601 and Prevents its Interaction with Glycoprotein VI, Integrin α2β1 and von Willebrand Factor. *J. Biol.*
602 *Chem.* **282**, 26928–26938 (2007).
603 32. Mathur, G. *et al.* Transgene-mediated suppression of dengue viruses in the salivary glands of the
604 yellow fever mosquito, Aedes aegypti. *Insect Mol. Biol.* **19**, 753–763 (2010).
605 33. Chagas, A. C. *et al.* Collagen-binding protein, Aegyptin, regulates probing time and blood feeding
606 success in the dengue vector mosquito, Aedes aegypti. *Proc. Natl. Acad. Sci. U. S. A.* **111**, 6946–
607 6951 (2014).
608 34. Tung, G. A. & Fonseca, D. M. Internal and external drivers interact to create highly dynamic
609 mosquito blood-feeding behaviour. *Proc. R. Soc. B Biol. Sci.* **291**, 20241105 (2024).
610 35. Hamel, R. *et al.* Biology of Zika Virus Infection in Human Skin Cells. *J. Virol.* **89**, 8880–8896 (2015).
611 36. Surasombatpattana, P. *et al.* Dengue virus replication in infected human keratinocytes leads to
612 activation of antiviral innate immune responses. *Infect. Genet. Evol.* **11**, 1664–1673 (2011).
613 37. Wichit, S. *et al.* Aedes Aegypti saliva enhances chikungunya virus replication in human skin
614 fibroblasts via inhibition of the type I interferon signaling pathway. *Infect. Genet. Evol. J. Mol.*
615 *Epidemiol. Evol. Genet. Infect. Dis.* **55**, 68–70 (2017).
616 38. Rossignol, P. A., Ribeiro, J. M. & Spielman, A. Increased intradermal probing time in sporozoite-
617 infected mosquitoes. *Am. J. Trop. Med. Hyg.* **33**, 17–20 (1984).
618 39. Yamamoto, D. S., Sumitani, M., Kasashima, K., Sezutsu, H. & Matsuoka, H. Inhibition of Malaria
619 Infection in Transgenic Anopheline Mosquitoes Lacking Salivary Gland Cells. *PLoS Pathog.* **12**,
620 e1005872 (2016).
621 40. Wei Xiang, B. W. *et al.* Dengue virus infection modifies mosquito blood-feeding behavior to increase
622 transmission to the host. *Proc. Natl. Acad. Sci. U. S. A.* **119**, e2117589119 (2022).

623 41. Alves e Silva, T. L. *et al.* High-Resolution Proteomics Unveils Salivary Gland Disruption and Saliva-
624 Hemolymph Protein Exchange in Plasmodium-Infected Mosquitoes. *bioRxiv* 2025.02.28.640873
625 (2025) doi:10.1101/2025.02.28.640873.
626 42. Bahr, L. *et al.* Antibody response to Aedes aegypti D7L1+2 salivary proteins as marker of aggregate
627 vector exposure and correlate of dengue virus susceptibility. *bioRxiv* (2025)
628 doi:https://doi.org/10.1101/2025.05.01.651659.
629 43. Lan, C. *et al.* Screening and analysis of immune-related genes of Aedes aegypti infected with
630 DENV2. *Acta Trop.* **236**, 106698 (2022).
631 44. Sim, S., Ramirez, J. L. & Dimopoulos, G. Dengue Virus Infection of the Aedes aegypti Salivary
632 Gland and Chemosensory Apparatus Induces Genes that Modulate Infection and Blood-Feeding
633 Behavior. *PLoS Pathog.* **8**, e1002631 (2012).
634 45. Tchankouo-Nguetcheu, S. *et al.* Infection by chikungunya virus modulates the expression of several
635 proteins in Aedes aegypti salivary glands. *Parasit. Vectors* **5**, 264 (2012).
636 46. Chisenhall, D. M. *et al.* Infection with dengue-2 virus alters proteins in naturally expectorated saliva
637 of Aedes aegypti mosquitoes. *Parasit. Vectors* **7**, 252 (2014).
638 47. Olmo, R. P. *et al.* Control of dengue virus in the midgut of Aedes aegypti by ectopic expression of
639 the dsRNA-binding protein Loqs2. *Nat. Microbiol.* **3**, 1385–1393 (2018).
640 48. Marois, E. *et al.* High-throughput sorting of mosquito larvae for laboratory studies and for future
641 vector control interventions. *Malar. J.* **11**, 1–9 (2012).
642 49. Patil, I. Visualizations with statistical details: The 'ggstatsplot' approach. *J. Open Source Softw.* **6**,
643 3167 (2021).
644 50. Xu, S. *et al.* Use ggbreak to Effectively Utilize Plotting Space to Deal With Large Datasets and
645 Outliers. *Front. Genet.* **12**, (2021).
646 51. Forster, B., Van De Ville, D., Berent, J., Sage, D. & Unser, M. Extended depth-of-focus for multi-
647 channel microscopy images: A complex wavelet approach. in *2004 2nd IEEE International*
648 *Symposium on Biomedical Imaging: Macro to Nano (IEEE Cat No. 04EX821)* vol. 2 660–663 (IEEE,
649 Arlington, VA, USA, 2004).
650

651 **Supplementary Materials**
652
653 **Supplementary Figures**
654
655 **Supplementary figure 1-** Establishment and phenotypic characterization of the Fudgel transgenic line.
656
657 **Supplementary figure 2-** Western Blot membranes for @V5-mTurq detection optimization.
658
659 **Supplementary figure 3-** Western Blot membranes of saliva samples upon different physiological
660 states.
661
662 **Supplementary figure 4-** Individual replicate plots for @V5-mTurq detection in saliva samples upon
663 different physiological states**.**
664
665 **Supplementary figure 5-** Fluorescent images of Fudgel salivary glands after natural blood-feeding or
666 forced salivation.
667
668 **Supplementary figure 6-** Western Blot membranes of saliva samples upon infection with ZIKV or
669 CHIKV.
670
671 **Supplementary Tables**
672
673 **Supplementary table 1-** Top 50 genes expressed in the distal lateral lobes (dll) of the salivary glands
674 and associated dll averaged UMAP score.
675
676 **Supplementary table 2-** Salivary glands lobes-specifically expressed genes and associated
677 abundance in saliva.
678
679 **Supplementary table 3-** Western Blot raw data for V5-mTurq signal detection by Western Blot.
680
681 **Supplementary table 4-** Western Blot raw data for V5-mTurq detection in saliva samples upon different
682 physiological states.
683
684 **Supplementary table 5-** Salivary glands fluorescence quantification raw values and CTCF calculations
685 for purging measurement after natural blood-feeding or forced salivation.
686
687 **Supplementary table 6-** Western Blot raw data for V5-mTurq detection in saliva samples upon ZIKV
688 and CHIKV infection.
689

690 **Supplementary table 7-** qPCR raw data for ZIKV, CHIKV and mTurq RNA detection in mosquitoes
691 carcasses.
692
693 **Supplementary table 8-** Primers used for Fudgel genetic construct cloning, transgene insertion
694 mapping and qPCR.
695
696 **Supplementary Video**
697
698 **Supplementary video 1-** Live V5-mTurq detection in a Fudgel female proboscis upon forced salivation
699 in PBS.
700